View metadata, citation and similar papers at core.ac.uk

brought to you by CORE

provided by Calhoun, Institutional Archive of the Naval Postgraduate School

Calhoun: The NPS Institutional Archive

Faculty and Researcher Publications

Faculty and Researcher Publications

2010-08

Spacecraft Proximity Navigation and Autonomous Assembly based on Augmented State Estimation: Analysis and Experiments

Calhoun is a project of the Dudley Knox Library at NPS, furthering the precepts and goals of open government and government transparency. All information contained herein has been approved for release by the NPS Public Affairs Officer.

Dudley Knox Library / Naval Postgraduate School
411 Dyer Road / 1 University Circle
Monterey, California USA 93943

http://www.nps.edu/library

AIAA Guidance, Navigation, and Control Conference
2 - 5 August 2010, Toronto, Ontario Canada

AIAA 2010-7756

Spacecraft Proximity Navigation and Autonomous Assembly based on Augmented State Estimation: Analysis and Experiments

Veronica Pellegrini[1]
University of California, Santa Cruz, CA

Riccardo Bevilacqua[2]
Rensselaer Polytechnic Institute, Troy, NY

Marcello Romano[3]
Naval Postgraduate School, Monterey, CA

and
Fabio Curti[4]
School of Aerospace Engineering, "Sapienza" University of Rome, Italy

This paper presents a spacecraft relative navigation scheme based on a tracking technique. The augmented state estimation technique is a variable-dimension filtering approach, originally introduced by Bar-Shalom and Birmiwal [1]. In this technique, the state model for a target spacecraft is augmented by introducing, as extra state components, the target's control inputs. The maneuver, modeled as accelerations, is estimated recursively along with the other states associated with position and velocity, while a target maneuvers. By using the proposed navigation method, a chaser spacecraft can estimate the relative position, the attitude and the control inputs of a target spacecraft, flying in its proximity. It is assumed that the chaser spacecraft is equipped with on-board sensors able to measure the relative position and relative attitude of the target spacecraft. The available sensors would provide a measurement update sample time of the order of one second and be subject to random measurement interruption longer than one second. As preliminary analysis, this work introduces the technique applied to the planar, three-degree-of-freedom, spacecraft

[1] Ph. D. Student, University of California, Santa Cruz, Department of Applied Mathematics and Statistics, Email: vpellegr@ucsc.edu.
[2] Assistant Professor, Department of Mechanical, Aerospace, and Nuclear Engineering, Email: bevilr@rpi.edu, AIAA Member.
[3] Associate Professor, Department of Mechanical and Aerospace Engineering, and Space Systems Academic Group, Email: mromano@nps.edu, AIAA Associate Fellow.
[4] Associate Professor, Scuola di Ingegneria Aerospaziale, Dipartimento di Ingegneria Aerospaziale e Astronautica, Email: fcurti@psm.uniroma1.it, AIAA Member.

This material is declared a work of the U.S. Government and is not subject to copyright protection in the United States.

relative motion. The proposed approach is validated via hardware-in-the-loop experimentation, using four autonomous three-degree-of-freedom robotic spacecraft simulators, floating on a flat floor. The proposed navigation method is proved to be more robust than a standard Kalman Filter estimating relative position and attitude only.

Nomenclature

ACRONYMS

IE = Input Estimation

LVLH = Local Vertical Local Horizontal Reference Frame centered on the Chaser Spacecraft

NPS = Naval Postgraduate School

SRL = Spacecraft Robotic Laboratory

DoF = Degree of Freedom of the System

STATE AND VARIABLES SYMBOLS

$\tilde{a}$ = Estimated State or Variable

k = Discrete Time Index

m = Number of Control Inputs

n = Dimension of the State vector

h = Number of variable observed

$\boldsymbol{X}_{rel}$ = Relative State vector between two S/C, $(13,1)$

${}^{C_j}_{T_i}\boldsymbol{S}$ = Complete i-th Target State vector ref to j-th Chaser S/C, (13,1)

${}^{C_j}_{T_i}\boldsymbol{X}$ = State vector of i–th Target S/C with respect to j-th Chaser S/C,

6DoF: $${}^{C_j}_{T_i}\boldsymbol{X} = {}^{C_j}_{T_i}\left[x \quad y \quad z \quad \dot{x} \quad \dot{y} \quad \dot{z}\right]^T,$$

3DoF: $${}^{C_j}_{T_i}\boldsymbol{X} = {}^{C_j}_{T_i}\left[x \quad y \quad \dot{x} \quad \dot{y}\right]^T$$

${}^{C_j}_{T_i}\boldsymbol{\Theta}$ = Attitude State vector of i–th Target S/C with respect to j-th Chaser S/C,

6DoF: ${}^{C_j}_{T_i}\boldsymbol{\Theta} = {}^{C_j}_{T_i}\left[q_{e1} \quad q_{e2} \quad q_{e3} \quad q_{e4} \quad \omega_{xT} \quad \omega_{yT} \quad \omega_{zT} \right]^T$,

3DoF: ${}^{C_j}_{T_i}\boldsymbol{\Theta} = {}^{C_j}_{T_i}\left[\theta \quad \dot{\theta} \right]^T$

${}^{C_j}_{T_i}\boldsymbol{X}_A = \begin{bmatrix} {}^{C_j}_{T_i}\boldsymbol{X} \\ \mathbf{u_T} \end{bmatrix}$ = Augmented State vector of i–th Target S/C with respect to j-th Chaser S/C

${}^{C_j}_{T_i}\boldsymbol{\Theta}_A = \begin{bmatrix} {}^{C_j}_{T_i}\boldsymbol{\Theta} \\ \boldsymbol{M_T} \end{bmatrix}$ = Augmented Attitude State vector of i–th Target S/C with respect. to j-th Chaser S/C,

${}^{C_j}_{T_i}B$ = Control Matrix referred of i-th Target S/C with respect to j-th Chaser S/C, (nxm)

${}^{C_j}_{T_i}B(k)$ = Discretized Control Matrix referred of i-th Target S/C with respect to j-th Chaser S/C, (nxm)

${}^{C_j}_{T_i}B_A(k)$ = Discretized Augmented Control Matrix referred of i-th Target S/C with respect to j-th Chaser S/C,

$((n+m)xm)$

${}^{C_j}_{T_i}F$ = Dynamical Matrix of i-th Target S/C with respect to j-th Chaser S/C, (nxn)

${}^{C_j}_{T_i}F_A$ = Augmented Dynamical Matrix of i-th Target S/C with respect to j-th Chaser S/C, $((n+m)x1)$

${}^{C_j}_{T_i}\Phi$ = Transition Matrix of the dynamics of the i-th Target S/C with respect to j-th Chaser S/C, (nxn)

${}^{C_j}_{T_i}\Phi_A$ = Augmented Transition Matrix of the dynamics of the i-th Target S/C with respect to j-th Chaser S/C,

$((n+m)xn)$

G = Input Noise matrix, (nxn): n is the dimension of the state vector

H = Measurement matrix, (hxn)

$G_A = \begin{bmatrix} G \\ 0_{mxn} \end{bmatrix}$ = Augmented Input Noise matrix

$H_A = \begin{bmatrix} H & 0_{hxm} \end{bmatrix}$ = Augmented Measurement matrix

Z = Measurement vector, $(hx1)$

$Z_A = \begin{bmatrix} Z \\ 0_{mx1} \end{bmatrix}$ = Augmented Measurement vector

$\boldsymbol{W}$ = Input noise vector, assumed to be Gaussian white zero mean with covariance Q_k, $(mx1)$

$\boldsymbol{V}$ = Measurement noise vector, assumed to be Gaussian white zero mean with covariance R_k, $(hx1)$

Q_k = Process noise covariance matrix, (nxn)

R_k = Measurement noise covariance matrix, $(hx1)$

$\boldsymbol{u}_C$ = Chaser's control vector, $(mx1)$

$\boldsymbol{u}_T$ = Target's control vector, $(mx1)$

$\boldsymbol{M}_C$ = Chaser spacecraft torque vector, $(mx1)$

$\boldsymbol{M}_T$ = Target spacecraft torque vector, $(mx1)$

P_0 = Initial state error covariance matrix, (nxn)

T_s = Sampling time

I_{axa} = Identity Matrix,

0_{bxc} = Zeros Matrix

i_C = Chaser Orbital Inclination

R_e = Earth Radius

$\begin{bmatrix} c & s & k \end{bmatrix}$ = Coefficients for the linearized J2 model for Satellite Formation Flight

$[\phi, \varphi, \psi]$ = Euler Angles

r_C = Chaser Altitude

ω_{orbC} = Chaser Orbital Angular Velocity

θ = Target Attitude angle in Chaser S/C body frame

$\dot{\theta}$ = Target Angular velocity in Chaser S/C body frame

$\begin{bmatrix} x & y & z \end{bmatrix}^T$ = Target Cartesian Coordinates in Chaser S/C body frame

$\begin{bmatrix} \dot{x} & \dot{y} & \dot{z} \end{bmatrix}^T$ = Target Linear Velocities in Chaser S/C body frame

${}^C\boldsymbol{\omega}_{rel} = {}^C R_T \, {}^T\boldsymbol{\omega}_T - {}^C\boldsymbol{\omega}_C$ = Relative Angular velocity between Target and Chaser S/C, in Chaser S/C body frame

${}^T\boldsymbol{\omega}_T = \begin{bmatrix} \omega_{xT} & \omega_{yT} & \omega_{zT} \end{bmatrix}^T$ = Target S/C angular velocities in Target S/C body frame

${}^C\boldsymbol{\omega}_C = \begin{bmatrix} \omega_{xC} & \omega_{yC} & \omega_{zC} \end{bmatrix}^T$ = Chaser S/C angular velocities in Chaser S/C body frame

${}^{C_j}_{T_i}\boldsymbol{Q}_e = {}^{C_j}_{T_i}\begin{bmatrix} q_{e1} & q_{e2} & q_{e3} & q_{e4} \end{bmatrix}^T$ = Quaternion of the attitude of the i-th Target S/C with respect to the j-th Chaser S/C

$\boldsymbol{q}_e = \begin{bmatrix} q_{e1} & q_{e2} & q_{e3} \end{bmatrix}^T$ = Vectorial components of ${}^{C_j}_{T_i}\boldsymbol{Q}_e$

$J = \begin{bmatrix} J_x & 0 & 0 \\ 0 & J_y & 0 \\ 0 & 0 & J_z \end{bmatrix}$ = S/C Inertial matrix of each S/C

$f()$ = General Function

${}^C R_T$ = Rotational matrix from Target S/C body frame to Chaser S/C body frame

${}^C R_T$ = Rotational matrix from Chaser S/C body frame to Target S/C body frame

I. Introduction

Many different filters for tracking a maneuvering target have been considered in the literature. Approaches based on Kalman filter include in the work of Singer [2], in which the target acceleration is modeled as a random process with known exponential autocorrelation.

The input estimation approach for tracking a maneuvering target is proposed by Chan, et al. [4]. In this approach, the magnitude of the acceleration is identified by the least-squares estimation when a maneuver is detected. The estimated acceleration is then used in conjunction with a standard Kalman filter to compensate the state estimate of the target. The standard filter alone is used during periods when no maneuver takes place. The variable-dimension filtering approach is proposed by Bar-Shalom, et al. [2, 5]. In this approach, the state model for the target is changed

by introducing extra state components, the target's accelerations. The maneuver, modeled as an acceleration, is estimated recursively along with other states associated with position and velocity while a target maneuvers. Bogler, et al. [3] used this method as an implementation on high maneuver target tracking with maneuver detection**.**

The input estimation filter and the variable-dimension filter are commonly used in view of their computational efficiency and tracking performance. Among IE techniques, the Augmented State estimation approach yields reasonable performance without constant acceleration or small sampling time assumptions. Furthermore, it not only provides fast initial convergence rate, but it can also track a maneuvering target with fairly good accuracy as mentioned by Khaloozadeh and Karsaz [7]. Bahari, et al. [9, 12] proposed an intelligent error covariance matrix resetting, by a fuzzy logic, necessary for high maneuvering target tracking, to improve the estimation of the target state.

In space applications, particularly in the spacecraft relative navigation for the autonomous rendezvous and assembly, each vehicle is both the target and the chaser for the other satellite/s. Here an additional challenge is considered: the frequent loss of communications for the data exchange when the application involves more than one spacecraft. If the data communication is not the way spacecraft to perform the relative navigation, a vision based system may be used. These types of sensors require the image processing and may result in low frequency measurement updates, especially for small spacecraft with limited computation capabilities. Such sensors suffer of problems such as limitations on the field of view and/or other spacecraft obstructing the view. Furthermore, in the spacecraft relative maneuvering, each vehicle does not usually know the other vehicles inputs, i.e. it does not possess the information about the maneuvers performed by its fellow spacecraft. This missing information needs to be reconstructed in the estimation scheme that would otherwise diverge quickly.

We here focus on the utilization of low frequency update and low cost sensors, such as Commercial Off-The-Shelve (COTS) devices. In particular, the spacecraft are envisioned to have the availability of range measurements and relative attitude measurements.

This work presents the design of a spacecraft relative navigation system based on the augmented state estimation technique. Robustness to frequent signal loss and/or darkening of the sensors is achieved. Furthermore, the suggested approach reconstructs the information of the other vehicles' maneuvers.

The planar three-degree-of-freedom relative estimation approach is developed, and tested via hardware-in-the-loop experimentation. The four spacecraft simulators of the Spacecraft Robotics Laboratory at the Naval Postgraduate School are used for the experimental testing.

For the experimental part of this work, two dynamics models for the filter are here considered: 1) the classical Kalman filtering technique, [13], in which the unknown input (the maneuver command) is modeled as a random process, and 2) the augmented state estimation technique, where the maneuver is estimated, using a Kalman filter scheme [13], in real time, as an additional variable in an augmented state vector.

Between the two approaches, the second one proves to be the most successful. It yields satisfactory performances without constant accelerations or small sampling time assumptions. Furthermore, it does not only provide fast initial convergence rate, but it can also track a maneuvering target with a good accuracy under casually loss of the data link and slow data rate, allowing the spacecraft to perform critical maneuvers such as the docking and the multi-vehicle assembly.

The successful results of the preliminary study here presented, pave the way for further implementation of the augmented state vector approach for the full six degrees of freedom spacecraft relative motion.

The paper is organized as follows. Section II presents the equations of the six-degree-of-freedom motion for the spacecraft relative maneuvering. Section III presents the equations of the motion for the spacecraft simulators (three degrees of freedom), and the augmented estimation approach for the planar case. Section IV is dedicated to the experimental validation of the proposed approach, and also shows a failed assembly maneuver, when the classical Kalman filtering navigation method is used. Section V concludes the paper.

II. S/C Relative Motion Dynamics and Problem Statement

In this section we provide the dynamics of spacecraft relative motion in the generic full six degrees of freedom case. In the end of the section the restriction of the state vector for the planar case is introduced.

The spacecraft relative motion in full six degrees of freedom encompasses both the relative translation and rotation. The dynamics of such motion can be represented in the compact form as:

$$\dot{\boldsymbol{X}}_{rel} = f\left(\dot{\boldsymbol{X}}_{rel}\right) + B\left(\dot{\boldsymbol{X}}_{rel}\right)\boldsymbol{u} \tag{1}$$

where

$$\boldsymbol{X}_{rel} = \begin{bmatrix} x & y & z & q_{1e} & q_{2e} & q_{3e} & q_{4e} & \dot{x} & \dot{y} & \dot{z} & (\omega_{xT} - \omega_{xC}) & (\omega_{yT} - \omega_{yC}) & (\omega_{zT} - \omega_{zC}) \end{bmatrix}^T \quad (2)$$

We are referring to a Local Vertical Local Horizontal (LVLH) reference frame that rotates with the orbital angular velocity ω_{orbC} . The origin of LVLH moves on a virtual orbit, conveniently chosen to remain in the vicinity of the maneuvering spacecraft. This point can also be chosen as coincident with one of the spacecraft .The x - axis points from the center of the Earth to the center of LVLH, while the y-axis is in the orbital plane in the direction of the motion along the orbit and perpendicular to the x-axis. The z-axis completes the right-handed LVLH frame.

The linearized J2 model for the satellite formation flight equations, proposed by Schweighart, S. A., and Sedgwick, J. R. in [6], that include the J2 perturbation, is used in this work for representing the relative dynamics,

$$\begin{aligned} &\ddot{x} - 2(\omega c)\dot{y} - (5c^2 - 2)\omega^2 x = u_x \\ &\ddot{y} - 2(\omega c)\dot{x} = u_y \\ &\ddot{z} + k^2 z = u_z \end{aligned} \quad (3)$$

with

$$\begin{aligned} &c = \sqrt{(1+s)}, \\ &s = \frac{2J_2 R_e^2}{8r_c^2}[1 + 3\cos(2i_c)], \\ &k = \omega_{orbC}\sqrt{(1+s)} + \frac{3J_2 \omega_{orbC} R_e^2}{2r_c^2}[\cos(i_C)] \end{aligned} \quad (4)$$

For the attitude, the well known Euler's dynamics govern each spacecraft orientation. In the following equation, *T* stands for the target and it can be replaced with *C* for the chaser, remembering that each vehicle is both target and chaser in the assembly scenario we are envisioning.

$$J^T\dot{\boldsymbol{\omega}}_i + {}^T\boldsymbol{\omega}_i^{\times} J^T\boldsymbol{\omega}_i = \boldsymbol{M}_i \rightarrow \begin{cases} \dot{\omega}_{xi} = -\left[\dfrac{J_z - J_y}{J_x}\right]\omega_{yi}\omega_{zi} + \dfrac{M_{xi}}{J_x}; \\ \dot{\omega}_{yi} = -\left[\dfrac{J_x - J_z}{J_y}\right]\omega_{xi}\omega_{zi} + \dfrac{M_{yi}}{J_y}; \\ \dot{\omega}_{zi} = -\left[\dfrac{J_y - J_x}{J_z}\right]\omega_{xi}\omega_{yi} + \dfrac{M_{zi}}{J_z}. \end{cases} \quad \text{with } i = T \text{ or } i = C \tag{5}$$

The equations of the relative quaternion kinematics are

$$\begin{aligned} \boldsymbol{q}_e &= \frac{1}{2}\left(q_{e4}\,{}^C\boldsymbol{\omega}_{rel} - {}^C\boldsymbol{\omega}_{rel}{}^{\times}\boldsymbol{q}_e\right), \\ \dot{q}_{e4} &= -\frac{1}{2}\,{}^C\boldsymbol{\omega}_{rel}\cdot\boldsymbol{q}_e, \end{aligned} \tag{6}$$

where

$${}^C\boldsymbol{\omega}_{rel}{}^{\times} = \begin{bmatrix} 0 & -\omega_{zrel} & \omega_{yrel} \\ \omega_{zrel} & 0 & -\omega_{xrel} \\ -\omega_{yrel} & \omega_{xrel} & 0 \end{bmatrix} \tag{7}$$

The goal of this work is to preliminarily provide a robust estimation scheme for the relative navigation of *n* spacecraft (with $n \geq 2$), in the planar, three degrees of freedom case. The limitation to the three-degree-of-freedom case addresses the orbital in-plane motion, when attitude is maneuvered only along the cross-track direction. In particular each j-th S/C of the system should be able to estimate, at a minimum, the following state vector:

$${}^{C_j}_{T_i}\boldsymbol{S} = {}^{C_j}_{T_i}\begin{bmatrix} x & y & \vartheta & \dot{x} & \dot{y} & \omega_{zT} \end{bmatrix} \tag{8}$$

Natural extension of this preliminary work will be the implementation of the augmented state vector estimation approach to the full six degrees of freedom case.

III. The Augmented State Estimation Method for a 3DOF Laboratory Experimentation

In this section, the theory for the NPS's three-degree-of-freedom S/C simulators is presented. The limitations to three degrees of freedom (two for the planar translation, and one for the rotation about the vertical axis) addresses the case of relative maneuvering when the cross-track motion is not considered and the attitude is constrained to one

axis. The relative dynamics is here chosen as a double integrator for the center of masses relative motion and for the orientation about the vertical axis, representing the reality of the NPS spacecraft simulators.

The acceleration is treated as an additional term in the corresponding state equation, so that the model will provide an augmentation in the state space, with the relative acceleration to be part of the estimation.

Assuming separate control for the attitude and the position allows for considering uncoupled dynamics, so that we can proceed as follows. We assume the target moving in a plane and that the state vector can be written as,

$$ {}^{C_j}_{T_i}\boldsymbol{X} = {}^{C_j}_{T_i}\begin{bmatrix} x & y & \dot{x} & \dot{y} \end{bmatrix}^T \tag{9} $$

The discrete dynamics for the problem is the following.

$$ \begin{aligned} &{}^{C_j}_{T_i}\boldsymbol{X}\left(k+1\right) = {}^{C_j}_{T_i}\Psi\left(k\right){}^{C_j}_{T_i}\boldsymbol{X}\left(k\right) + {}^{C_j}_{T_i}B\left(k\right)\left(\boldsymbol{u}_T(k) - \boldsymbol{u}_C(k)\right) + G\boldsymbol{W}\left(k\right), \\ &Z\left(k\right) = H\,{}^{C_j}_{T_i}\boldsymbol{X}\left(k\right) + \boldsymbol{V}\left(k\right), \end{aligned} \tag{10} $$

The expressions of the matrices: G, H, ${}^{C_j}_{T_i}B\left(k\right)$, and Φ as functions of the measurement update time T_s for this planar case can be written as,

$$ \begin{aligned} &G = I_{4x4}, \qquad \mathrm{H} = \begin{pmatrix} I_{2x2} & 0_{2x2} \end{pmatrix}, \qquad {}^{C_j}_{T_i}B\left(k\right) = \int_0^{T_s}\left({}^{C_j}_{T_i}\Phi\left(t\right)\cdot {}^{C_j}_{T_i}B\right)dt = \begin{pmatrix} \frac{T_s^2}{2} & 0 \\ 0 & \frac{T_s^2}{2} \\ T_s & 0 \\ 0 & T_s \end{pmatrix} / m_{sc}, \\ &{}^{C_j}_{T_i}\Psi\left(k\right) = {}^{C_j}_{T_i}\Phi\left(T_s\right) = e^{{}^{C_j}_{T_i}FT_S} = I_{4x4} + {}^{C_j}_{T_i}FT_s + {}^{C_j}_{T_i}F\frac{T_s^2}{2} + \ldots = \begin{pmatrix} 1 & 0 & T_s & 0 \\ 0 & 1 & 0 & T_s \\ 0 & 0 & 1 & 0 \\ 0 & 0 & 0 & 1 \end{pmatrix}, \end{aligned} \tag{11} $$

being

$$ \boldsymbol{F} = \begin{pmatrix} 1 & 0 & 0 & 0 \\ 0 & 1 & 0 & 0 \\ 0 & 0 & 0 & 0 \\ 0 & 0 & 0 & 0 \end{pmatrix}, \qquad B = \begin{pmatrix} I_{2x2} \\ 0_{2x2} \end{pmatrix} / m_{sc}. \tag{12} $$

The augmented dynamics and related state equation matrices can be written as,

$$
\begin{aligned}
&{}^{C_j}_{T_i}\boldsymbol{X}_A = \begin{bmatrix} {}^{C_j}_{T_i}\boldsymbol{X}(k+1) \\ \boldsymbol{u}_T(k+1) \end{bmatrix} = {}^{C_j}_{T_i}\Psi_A(k) \begin{bmatrix} {}^{C_j}_{T_i}\boldsymbol{X}(k) \\ \boldsymbol{u}_T(k) \end{bmatrix} + G_A \boldsymbol{W}(k) + {}^{C_j}_{T_i}B_C(k)\boldsymbol{u}_C(k), \\
&Z_A(k) = H_A \begin{bmatrix} {}^{C_j}_{T_i}\boldsymbol{X}(k) \\ \boldsymbol{u}_T(k) \end{bmatrix} + \boldsymbol{V}(k), \\
&G_A = \begin{pmatrix} G \\ 0_{2x4} \end{pmatrix}, \quad H_A = \begin{pmatrix} I_{2x2} & 0_{2x4} \end{pmatrix}, \qquad {}^{C_j}_{T_i}B_C = \begin{pmatrix} 0 & 0 \\ 0 & 0 \\ -1 & 0 \\ 0 & -1 \\ 0 & 0 \\ 0 & 0 \end{pmatrix} / m_{SC}, \boldsymbol{u}_C = \begin{bmatrix} u_{Cx} \\ u_{Cy} \end{bmatrix}, \\
&{}^{C_j}_{T_i}\Psi_A(k) = \begin{pmatrix} {}^{C_j}_{T_i}\Psi(k) & {}^{C_j}_{T_i}B(k) \\ 0_{2x4} & I_{2x2} \end{pmatrix} = \begin{pmatrix} 1 & 0 & T_S & 0 & \frac{T_S^2}{2m_{SC}} & 0 \\ 0 & 1 & 0 & T_S & 0 & \frac{T_S^2}{2m_{SC}} \\ 0 & 0 & 1 & 0 & \frac{T_S}{m_{SC}} & 0 \\ 0 & 0 & 0 & 0 & 0 & \frac{T_S}{m_{SC}} \\ 0 & 0 & 0 & 0 & 1 & 0 \\ 0 & 0 & 0 & 0 & 0 & 1 \end{pmatrix}, \\
&{}^{C_j}_{T_i}B_C(k) = \int_0^{T_s} \left({}^{C_j}_{T_i}\Phi_A(t) \cdot {}^{C_j}_{T_i}B_C \right) dt = \begin{pmatrix} -\frac{T_s^2}{2} & 0 \\ 0 & -\frac{T_s^2}{2} \\ -T_S & 0 \\ 0 & -T_S \\ 0 & 0 \\ 0 & 0 \end{pmatrix} / m_{sc}.
\end{aligned}
\tag{13}
$$

The same algorithm is implemented for target's attitude and control torque estimation. Assuming the target rotating only around the vertical axis (z-axis), the i-th Target attitude state vector, with respect to the j-th Chaser spacecraft, is chosen to be,

$$
{}^{C_j}_{T_i}\boldsymbol{\Theta} = {}^{C_j}_{T_i}\begin{bmatrix} \theta & \dot{\theta} \end{bmatrix}^T, \tag{14}
$$

The discrete dynamics for the attitude problem is

$$
\begin{aligned}
&{}^{C_j}_{T_i}\boldsymbol{\Theta}(k+1) = {}^{C_j}_{T_i}\Psi(k)\,{}^{C_j}_{T_i}\boldsymbol{\Theta}(k) + {}^{C_j}_{T_i}B(k)(\boldsymbol{M}_T(k) - \boldsymbol{M}_C(k)) + G\boldsymbol{W}(k),\\
&Z(k) = H\,{}^{C_j}_{T_i}\boldsymbol{\Theta}(k) + \boldsymbol{V}(k),
\end{aligned}
\tag{15}
$$

and the principal dynamics matrices, as function of the time sampling T_S, are

$$
\begin{aligned}
&G = I_{2x2}, \qquad H = \begin{pmatrix}1 & 0\end{pmatrix}, \qquad {}^{C_j}_{T_i}B(k) = \int_0^{T_s}\left({}^{C_j}_{T_i}\Phi(t)\cdot {}^{C_j}_{T_i}B\right)dt = \begin{pmatrix}\dfrac{T_s^2}{2J_{z/sc}}\\[2ex] \dfrac{T_s}{J_{z/sc}}\end{pmatrix} / J_{sc},\\
&{}^{C_j}_{T_i}\Psi(k) = {}^{C_j}_{T_i}\Phi(T_s) = e^{{}^{C_j}_{T_i}FT_S} = I_{2x2} + {}^{C_j}_{T_i}FT_s + {}^{C_j}_{T_i}F\frac{T_s^2}{2} + \ldots = \begin{pmatrix}1 & Ts\\ 0 & 1\end{pmatrix},
\end{aligned}
\tag{16}
$$

being

$$
{}^{C_j}_{T_i}F = \begin{pmatrix}0 & 1\\ 0 & 0\end{pmatrix},\ {}^{C_j}_{T_i}B = \begin{pmatrix}0\\ 1\end{pmatrix} / J_{z/sc}.
\tag{17}
$$

The formulation of the augmented state dynamics can be written as,

$$
{}^{C_j}_{T_i}\boldsymbol{\Theta}_A(k)=\begin{bmatrix}{}^{C_j}_{T_i}\boldsymbol{\Theta}(k+1)\\ \boldsymbol{M}_T(k+1)\end{bmatrix}={}^{C_j}_{T_i}\Psi_A(k)\begin{bmatrix}{}^{C_j}_{T_i}\boldsymbol{\Theta}(k)\\ \boldsymbol{M}_T(k)\end{bmatrix}+{}^{C_j}_{T_i}B_C(k)\boldsymbol{M}_c+G_A\boldsymbol{W}(k),
$$

$$
Z_A(k)=H_A\begin{bmatrix}{}^{C_j}_{T_i}\boldsymbol{\Theta}(k)\\ \boldsymbol{M}_T(k)\end{bmatrix}+\boldsymbol{V}(k),
$$

$$
G_A=\begin{pmatrix}G\\ 0_{2x2}\end{pmatrix},\quad H_A=\begin{pmatrix}1 & 0 & 0\end{pmatrix},\qquad {}^{C_j}_{T_i}B_C=\begin{pmatrix}0\\ -1\\ 0\end{pmatrix}/J_{z/sc},\qquad \boldsymbol{M}_c=\begin{bmatrix}M_z\end{bmatrix}
$$

$$
{}^{C_j}_{T_i}B_C(k)=\int_0^{T_s}\left({}^{C_j}_{T_i}\Phi(t)\cdot{}^{C_j}_{T_i}B_C\right)dt=\begin{pmatrix}-T_s\\ -\dfrac{T_s^2}{2}\\ 0\end{pmatrix}/J_{z/sc},
$$

$$
{}^{C_j}_{T_i}\Psi_A(k)=\begin{pmatrix}{}^{C_j}_{T_i}\Psi(k) & {}^{C_j}_{T_i}B(k)\\ 0_{2x2} & I_{2x2}\end{pmatrix}=\begin{pmatrix}1 & T_s & \dfrac{T_s^2}{2J_{z/sc}}\\ 0 & 1 & \dfrac{T_s^2}{J_{z/sc}}\\ 0 & 0 & 1\end{pmatrix}. \tag{18}
$$

IV. Experimental Results: Augmented State Estimation employed for Multi-Spacecraft Assembly

In this section, assembly maneuvers are employed to experimentally test the suggested relative navigation scheme. In particular, the guidance and control parts of the experiments are the same presented by Bevilacqua et al. in the AIAA GNC 2009 ([11]).

For our simulation we do not implement collision avoidance algorithm, however the control has been previously successfully tested [14].

The four spacecraft simulators available at NPS are three-degree-of-freedom robots, moving frictionless on a very flat epoxy floor, using linear air bearings (see Fig. 1). They are powered by eight body fixed compressed air thrusters, and equipped with sensors and on board computer of similar dynamics and performances of what found on a real small spacecraft. In particular, the onboard actuators are on/off thrusters, capable of producing a single force value when on. Schmitt Trigger and Pulse Width Modulation are used, in order to accurately track continuous control signals with on/off devices. The continuous controls are generated by the onboard control system, based on the approach of Ref. [11]. For details on the hardware, refer to [10].

At this stage the simulators do not have hardware dedicated to relative measurements. Relative measurement is obtained by exploiting the ad-hoc wireless communication ([10]). This feature has the benefit of flexibility in imposing the desired frequency of measurement update, by simple modification of the software.

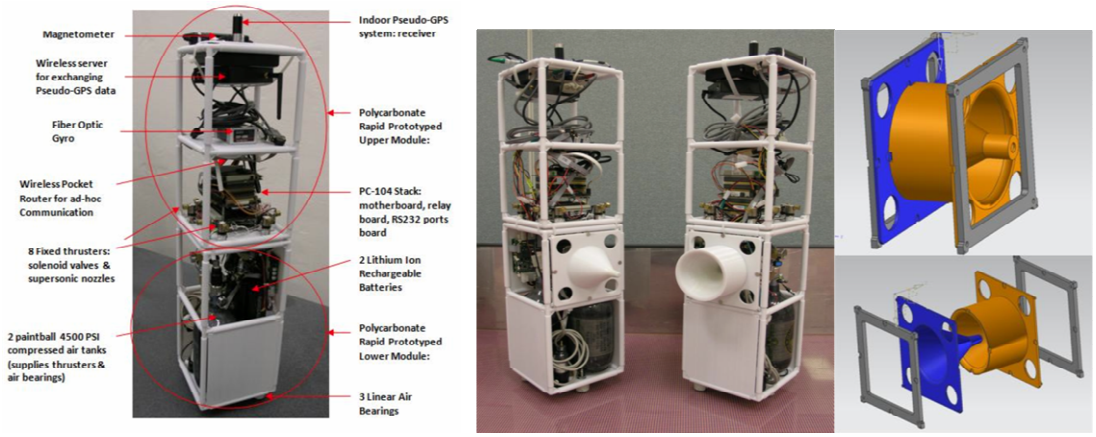

Fig. 1 Spacecraft Simulators and Docking Interfaces, Spacecraft Robotics Laboratory, Naval Postgraduate School.

Two experimental runs are presented. The first one demonstrates the unsuccessful relative navigation when classical Kalman Filtering is employed, considering the other S/C's maneuvers as a random process. Only two simulators are involved. The second experiment involves the four vehicles, showing how augmented state estimation can handle low measurement updates and unpredictable interruptions of updates, and still perform correct relative navigation, driving the mission to success.

In particular, we are here imposing, via the wireless network, an update of 2 seconds.

For the first part of the simulation each vehicle is chaser and target, there is complete symmetry, and each one knows, every two seconds the relative state vector of its target.

Once the two couple of robots are docked, each of the assembled structure is considered to be a new vehicle with new mass and geometry. For this reason the augmented state estimator is re-inizalized for the new structure with different mass and inertia as in Tab. 1. For this part of the simulation the software is running only on board the master S/C that is one for each couple.

Experimental Parameters		
Mass of each S/C	10,5	Kg
Inertia of Simulator	0.063	Kg m^2
Inertia of the two S/C assembled structure	0.18	Kg m^2
Single Thruster Estimated Force [17]	0.16	N
Docking Cone Semi-aperture	0.75	Degrees
Force arms (for torque generation)	5, 10, 21	Cm
Limit distance for switching off the thrusters	0.7	M
iGPS Accuracy	1	Mm
Gyroscope Accuracy	0.003	deg/sec

Tab.1 Main simulation parameters.

Q	$(1x10^{-6}) \cdot I_{6x6}$	Process Covariance Matrix, for the Adapted augmented state filter
R	$(1x10^{-4}) \cdot I_{2x2}$	Measurements Covariance Matrix, for the Adapted augmented state filter
Po	$R_k \cdot I_{6x6}$	Initial Covariance Matrix, for the Adapted augmented state filter
Ts	0.02 sec	Simulation Sampling Time

Tab.2 Position, Augmented State Filter parameters.

Q	$(1x10^{-12}) \cdot I_{3x3}$	Process Covariance Matrix, for the Adapted augmented state filter
R	$(1x10^{-2})$	Measurements Covariance Matrix, for the Adapted augmented state filter
Po	$R_k \cdot I_{3x3}$	Initial Covariance Matrix, for the Adapted augmented state filter
Ts	0.02 sec	Simulation Sampling Time

Tab.3 Attitude, Augmented State Filter parameters.

A. The classical Kalman filter technique

Fig. 2 is the bird's eye view of the experiment, demonstrating the unfeasibility of classical Kalman filter for spacecraft relative navigation. Two spacecraft simulators start maneuvering, with the goal of docking, from a short distance. The sides opposite to the bolded lines are the designated docking sides. After approximately 1 minute of maneuver, the accumulated error in relative state vector (position) exceeds the tolerance of the docking interfaces (Fig. 1), driving the vehicles into a failed docking maneuver. A video of the experiment can be found online at [16].

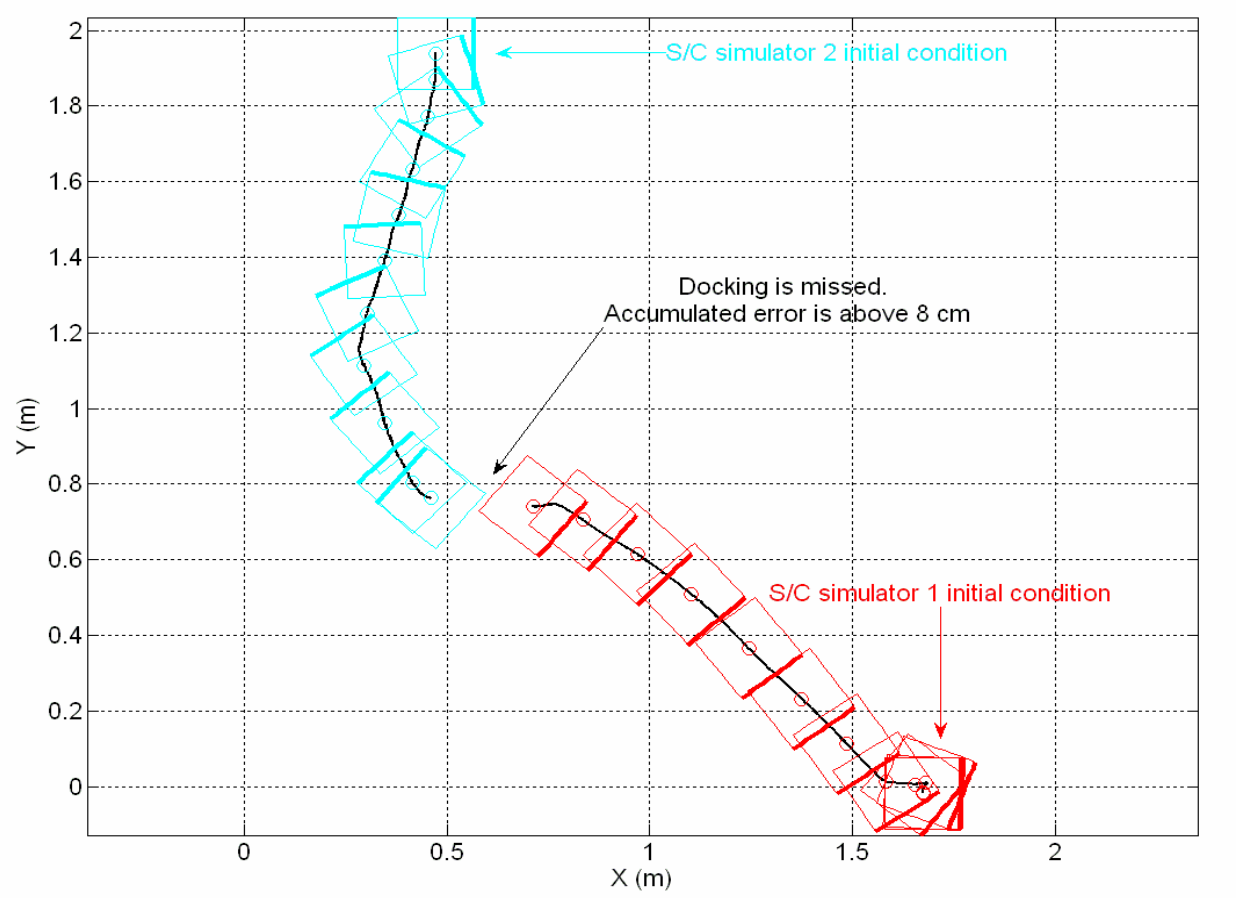

Fig. 2 Experimental Result: bird's eye view for two spacecraft simulator failed assembly maneuver. The relative navigation is performed via classical Kalman Filtering, no Input Estimation. The bolded lines are employed to help visualize the simulator's orientation.

B. The augmented state estimation technique

Fig. 3 is the bird's eye view of the experiment, demonstrating the feasibility of the augmented state estimation for spacecraft relative navigation. The main data for the filters are presented in Tab. 2, and 3. Four spacecraft simulators start maneuvering, with the goal of assembling into a line-shaped structure, from short distances. The sides opposite to the bolded lines are the designated docking sides. After less than 3 minutes of maneuver, the four vehicles successfully complete the given mission. The rectangular black and blue vehicles represent two spacecraft simulators docked and maneuvering as a single bigger unit. A video of the experiment can be found online at [17].

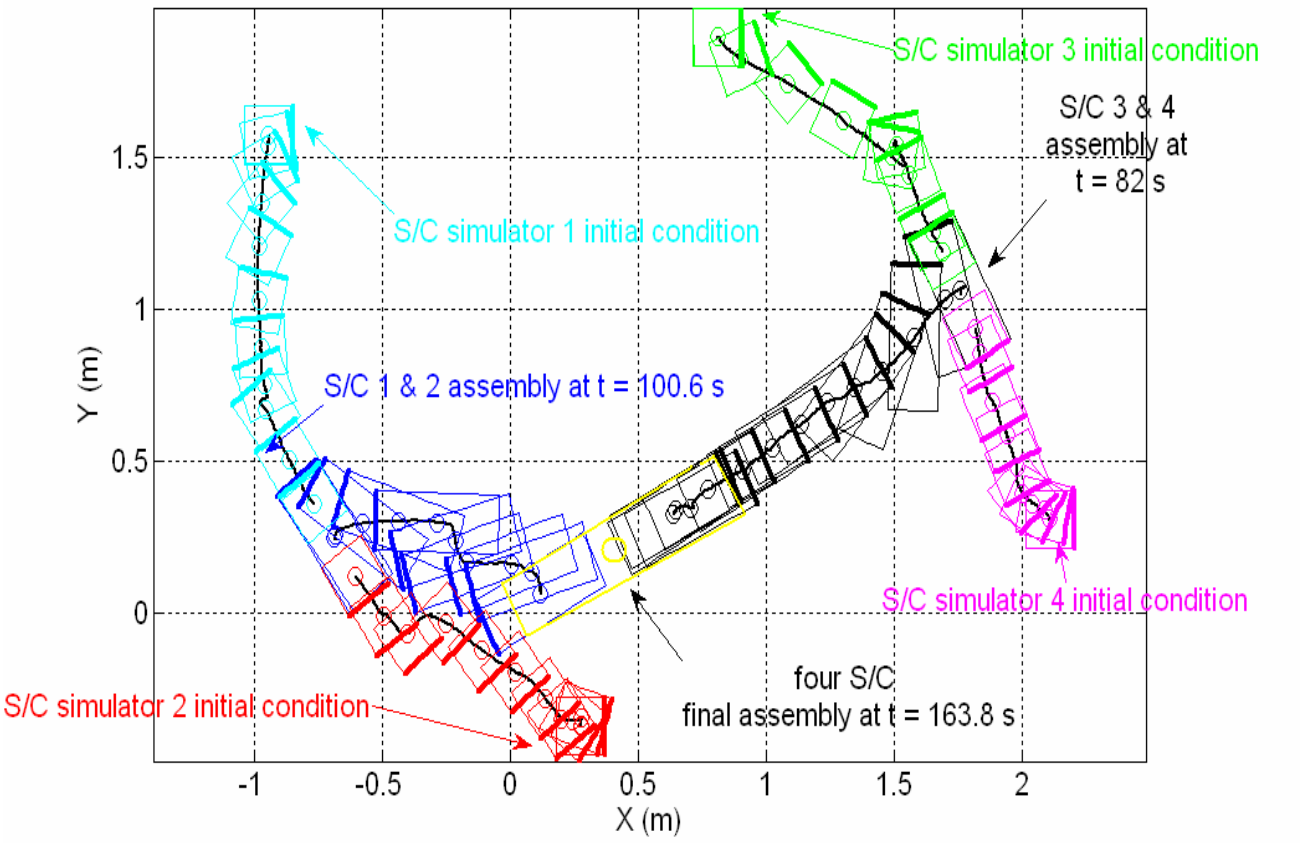

Fig. 3 Experimental Result: bird's eye view for four spacecraft simulator assembly maneuver. The relative navigation is performed via augmented state estimation. The bolded lines are employed to help visualize the simulator's orientation.

Once the simulators are assembled in couples, they maneuver as a single bigger unit, as described in [11]. In particular, the augmented state estimation is re-initialized in order to switch to a new target vehicle in terms of relative navigation.

V. Conclusion

In this work we are suggesting the employment of the augmented state estimation technique as the scheme for multiple spacecraft relative navigation. Theoretical developments are presented for the three-degree-of-freedom case, considering a planar motion for the relative position and a single axis of rotation for the laboratory implementation.

The experimental validation of the proposed methodology is presented, via floating spacecraft simulators, using an assembly maneuver as baseline. Experiments show how the augmented state estimation can cope with low frequency measurement updates, correctly performing the relative navigation, driving the mission to success. On the

other hand, Classical Kalman Estimation [13], is not accurate for close distances with low frequency measurement updates as demonstrated in the three-degree-of-freedom experimental section.

Following work will include extension of the proposed methodology to the six degrees of freedom full motion.

Acknowledgments

This research was performed while Dr. Bevilacqua was holding a National Research Council Research Associateship Award at the Spacecraft Robotics Laboratory of the US Naval Postgraduate School.

References

[1] Bar-Shalom, Y., Birmiwal K., "Variable dimension filtering for maneuvering target tracking," *IEEE Trans. Aerosp. Eletron. System,* Vol. 18, No. 15, 1982, pp. 621-567.

[2] Singer, R.A., "Estimating optimal tracking filter performance for manned maneuvering targets," *IEEE Trans. Aerosp. Electron. Syst.,* AES-6, 1970, pp. 473-483.

[3] Bogler, P. L., "Tracking a Maneuvering Target Using Input Estimation," *IEEE Transactions on Aerospace and Electronic Systems,* Vol. AES-23, issue 3, May, 1987, pp. 298-310.

[4] Chan, Y. T., Couture, F., "Maneuver detection and tracking correction by input estimation," *IEEE Proc. F,* 1993, Vol. 140, No. 1, pp. 21-28.

[5] Bar-Shalom, Y., X.Rong Li and Thiagalingam Kirubarajan, *Estimation with applications to tracking and navigation,* John Wiley & Sons INC, 2001, pp 199-287.

[6] Schweighart, S. A., and Sedgwick, J. R., "High-Fidelity Linearized J2 Model for Satellite Formation Flight," *Journal of Guidance, Control, and Dynamics,* Vol. 25, No. 6, Nov-Dec 2002, pp. 1073-1080.

[7] Khaloozadeh, H., Karsaz, A., "A new state augmentation for maneuvering targets detection," *Int. Conf. Signal Processing and Communications,* IEEE-SPCOM, 2004, pp. 65-69.

[8] Romano, M., Friedman, D.A., Shay, T.J., "Laboratory Experimentation of Autonomous Spacecraft Approach and Docking to a Collaborative Target," AIAA Journal of Spacecraft and Rockets, Vol. 44, No. 1, pp. 164-173, January-February 2007.

[9] Bahari, M. H., Karsaz, A., and Naghibi-S., M. B., "Intelligent Error Covariance Matrix Resetting for Maneuvering Target Tracking," *Journal of Applied Science,* Vol. 8, No. 12, 2008, pp. 2279-2285.

[10] Bevilacqua, R., Hall, J., Horning, J., Romano, M, "Ad-hoc wireless networking and shared computation based upon linux for autonomous multi-robot systems", *AIAA Journal of Aerospace Computing, Information, and Communication*, Vol.6 no.5, May, 2009, pp.328-353.

[11] Bevilacqua, R., Caprari, A., Hall, J. S., Romano, M., "Laboratory Experimentation of Multiple Spacecraft Autonomous Assembly," *AIAA Guidance, Navigation and Control Conference and Exhibit*, Chicago, Illinois, August 2009. AIAA-2009-6290.

[12] Bahari, M. H., and Pariz, N., "High maneuvering target tracking using an input estimation technique associated with fuzzy forgetting factor," *Scientific Research and Essay,* Vol.4, No. 10, October, 2009, pp. 936-945.

[13] Paul Zarchan, and Howard Musoff, *Fundamental of Kalman Filtering: A Practical Approach*, American Institute of Aeronautics and Astronautics INC, 2009, pp. 549-585.

[14] Bevilacqua, R., Lehmann, T., Romano, M., "Development and Experimentation of a LQR/APF Control for Autonomous Proximity Maneuvers of Multiple Spacecraft," accepted for publication on the *Elsevier Acta Astronautica*. To appear.

[15] Lugini, C., Romano, M., "A Ballistic-Pendulum Test Stand to Characterize Small Cold-gas Thruster Nozzles", *Acta Astronautica*, Vol. 64, No. 5-6, March-April, 2009, pp. 615-625.

[16] http://aa.nps.edu/~mromano/Movies4Web/GNC10_Video1.flv

[17] http://aa.nps.edu/~mromano/Movies4Web/GNC10_Video2.flv